

# A novel geometric error identification and prediction approach

Jinwei Fan, Peitong Wang \*, Zhuang Li

College of Mechanical Engineering & Applied Electronics Technology, Beijing University of Technology, Beijing 100124, China

**Abstract.** This paper proposed an integrated geometric error identification and prediction method to solve the uncertainty problem of the PDGEs of rotary axis. First, based on homogeneous transform matrix (HTM) and multi-body system (MBS) theory, The transfer matrix only considering the C-axes rotated is derived to the position error model. Then a geometric errors identification of rotary axis is introduced by measuring the error increment in three directions. Meanwhile the geometric errors of C-axis are described as truncated Fourier polynomials caused by fitting discrete values. Thus, The geometric error identification is converted into the function coefficient. Finally, the proposed new prediction and identification model of PDGEs in the global frame are verified through simulation and experiments with double ball-bar tests.

**Keywords** Geometric error identification, Prediction, Rotary axis, Double ball bar, Five-axis machine tool

## 1. Introduction

Five-axis CNC machine tools provide greater productivity, better flexibility, and less fixture time than three axis machining centers, because the cutting tool can approach the workpiece from any direction. However, the two rotary axes would bring in additional geometric errors subsequently, such as squareness between a rotary axis and a translational axis [1]. Therefore, an accurate and efficient measurement method of geometric errors is a key prerequisite for the improvement of five-axis machine tool accuracy [2]. If there is an effective method to improve or compensate for those deviations, the machining performance of multi-axis machines will be improved drastically.

In the past decades, some researches have been taken to measure and identify the errors that are inherent to a rotary axis of a multi-axis machine tool. Tsutsumi and Saito proposed a calibration method using the simultaneous four-axis control technique for five-axis machining centers with a tilting rotary table. The eight deviations were estimated by the observation equations from the ball bar measured results [3]. Zargarbashi identified eight link errors of a five-axis machine through measuring the tool center position deviations at a number of five-axis poses by using a ball-bar sensor [4]. Zargarbashi and Mayer presented a method consisting of five double ball bar tests to evaluate five trunnion axis motion errors including axial, radial and tilt errors.

However, some others may have such a capacity, require complex mathematical formulations and especially involve a complicated measurement process to identify the error parameters at present. Therefore, in this paper, a

novel prediction approach for geometric errors of rotary axis is proposed, which is effective and uncomplicated to improve the accuracy of identification.

## 2. Description of geometric errors

Geometric errors caused mainly by manufacturing and assembly defects are considered to be systematic errors. The geometric errors are usually categorized as position-independent geometric errors (PIGs) and position-dependent geometric errors (PDGEs). PDGEs have a certain relationship to the machine positions, while PIGs are constant values which are usually produced during the assembly process[10].  $\delta_x(C)$ ,  $\delta_y(C)$ ,  $\delta_z(C)$ ,  $\varepsilon_x(C)$ ,

$\varepsilon_y(C)$ ,  $\varepsilon_z(C)$  are position-dependent geometric errors of C-axis. The position -dependent geometric errors is fitted as the truncated Fourier polynomial as shown in Eq.(1). The fitting method includes Fourier polynomial, simple polynomial, Legendre polynomial, Chebyshev polynomial and so on. Compared to truncated Fourier polynomial, The random unpredictability of the error can be reflected, and the lower and upper limits of the position-dependent geometric satisfy the Dirichlet condition. Hence, the truncated Fourier polynomials is introduced to fit the PDGs. In this paper, error identification of rotary axis is the focus of research and the position-dependent geometric errors of rotary axis can be fully expressed in Eq.(1)

$$f(\theta) = \sum_{i=1}^n A_i \sin \frac{\theta}{2i-1} \quad 1$$

\* Corresponding author: 504789981@qq.com

Where  $f(\theta)$  and  $\theta$  denote geometric errors function and angles of rotation respectively.  $A_i$  represent a set of the coefficients for function.

### 3. Experiment and identify geometric errors of rotary axis

The identification and experiment of rotating axis geometric error are introduced in this paper. In previous studies, the identification of translational axis geometric error has been clearly specified, but the identification of rotating axis error has not been clearly specified. The geometric errors of rotary axis can be detected using renishaw XR20W double ball bar device. The remaining 10 PDGs can be derived from the multi-body theory and the Houston transformation matrix which contains six the linear errors and four angle errors. In order to express more briefly, the five PDGs of C-axis are identified by using DBB, which is taken as an example of rotary axis.

#### 3.1 Measurement

The detection of the C axis is divided into three models: C-X, C-Y and C-Z. The detection mode of the cue meter is detected in the X, Y and Z directions respectively. As shown in Fig.1, assuming  $P_c$  is the ideal origin of C axis coordinates,  $P'_c$  is the projection of the actual position of the far point of C axis coordinate system in the XZ plane,  $\Delta x$  is the projection of the positioning error of C axis in the x direction,  $\Delta$  is the projection of the degree error of C axis in the XZ plane. The PDGs of the C-axis will inevitably lead to the error of the position of different height points of the C axis in the X direction. During the measurement, firstly to ensure the accuracy of the experiment, the angle of B and C of the double pendulum head should be kept at  $0^\circ$  in the initial stage. Then when the C axis is rotated, the length of the measuring rod will change in the X,Y and Z directions. Two measuring points ( $c_1, c_2$ ) need to be selected that affects the accuracy of geometric error element parameters, as shown in Fig2 and Fig. 3. Finally the geometric error parameters of the C axis are deduced through the position relationship. It is obvious that the main objective of this experiment is to measure the values of delta L in the X,Y, and Z directions of  $c_1$  and  $c_2$ .

$$\Delta L_c = [\Delta L_{cx} \quad \Delta L_{cy} \quad \Delta L_{cz}]^T \quad 2$$

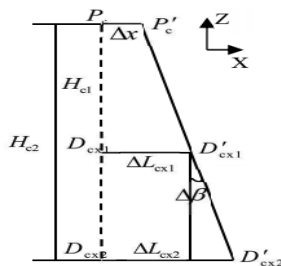


Fig.1 C-X measurement mode error generation mechanism

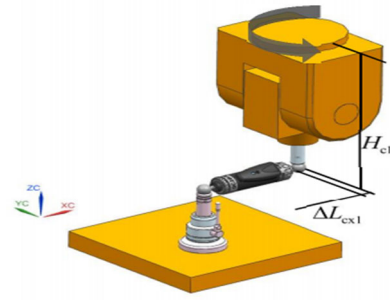


Fig.2 C-X-1 model

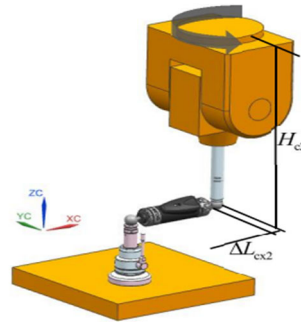


Fig.3 C-X-2 model

The ideal point  $D_{cx}$  and actual point  $D'_{cx}$  can be calculated from the HTM above Section 2. Therefore, the error increment of the length ( $\Delta L_{cx}$ ) of the measuring instrument in the X direction can be expressed as

$$\Delta L_{cx} = D'_{cx} - D_{cx} \quad 3$$

$$D_{cx} = \begin{bmatrix} \cos(c) & -\sin(c) & 0 & 0 \\ \sin(c) & \cos(c) & 0 & 0 \\ 0 & 0 & 1 & 0 \\ 0 & 0 & 0 & 1 \end{bmatrix} \begin{bmatrix} 0 \\ 0 \\ -H_c \\ 1 \end{bmatrix} \quad 4$$

$$D'_{cx} = \begin{bmatrix} 1 & 0 & S_{xc} & 0 \\ 0 & 1 & -S_{yc} & 0 \\ -S_{xc} & S_{yc} & 1 & 0 \\ 0 & 0 & 0 & 1 \end{bmatrix} \begin{bmatrix} \cos(c) & -\sin(c) & 0 & 0 \\ \sin(c) & \cos(c) & 0 & 0 \\ 0 & 0 & 1 & 0 \\ 0 & 0 & 0 & 1 \end{bmatrix} \begin{bmatrix} 1 & -\xi_z(c) & \xi_y(c) & \delta_x(c) \\ \xi_z(c) & 1 & -\xi_x(c) & \delta_y(c) \\ -\xi_x(c) & \xi_z(c) & 1 & \delta_z(c) \\ 0 & 0 & 0 & 1 \end{bmatrix} \quad 5$$

If Eq.(11) and Eq.(12) are put into Eq(10), the result of described

simplification will be

$$\begin{bmatrix} \cos(c) & -\sin(c) & -H_{c1} \cos(c) & -H_{c1} \sin(c) \\ \sin(c) & \cos(c) & -H_{c2} \cos(c) & -H_{c2} \sin(c) \\ 0 & 0 & 1 & 0 \\ 0 & 0 & 0 & 1 \end{bmatrix} \begin{bmatrix} \delta_x(c) \\ \delta_y(c) \\ \xi_y(c) \\ \xi_z(c) \end{bmatrix} = \begin{bmatrix} \Delta L_{cx1} + H_{c1} S_{xc} + H_{c1} \sin(c) S_{zc} \\ \Delta L_{cx2} + H_{c2} S_{xc} + H_{c2} \sin(c) S_{zc} \end{bmatrix} \quad 6$$

It is obvious that the matrix equation possesses four unknown parameters and the rank of coefficient matrix can be determined as 2. Considering the error source parameters unsolved in the matrix equation, another dimension matrix equation needs to be established which can identify the geometric error parameters. Therefore,

the error relationship needs to be confirmed in the C-Y direction.

(2) C-Y measurement

Similarly, the implementation of C-Y measurement is same to C-X measurement. During the measurement process,  $\Delta L_{cy1}$  and  $\Delta L_{cy2}$  need to be identified respectively. By combining Eq.10 and Eq.15, the error parameters  $(\delta_x(c), \delta_y(c), \xi_x(c), \xi_y(c))$  concerning the position of the four terms of the C-axis. C-Y measurement can be inversely solved.

$$\Delta L_{cy} = D'_{cy} - D_{cy} \quad 7$$

$$\begin{bmatrix} \cos(c) & -\sin(c) & -H_{c1}\cos(c) & -H_{c1}\sin(c) \\ \cos(c) & -\sin(c) & -H_{c2}\cos(c) & -H_{c2}\sin(c) \\ \sin(c) & \cos(c) & -H_{c1}\sin(c) & H_{c1}\cos(c) \\ \sin(c) & \cos(c) & -H_{c2}\sin(c) & H_{c2}\cos(c) \end{bmatrix} \begin{bmatrix} \delta_x(c) \\ \delta_y(c) \\ \xi_x(c) \\ \xi_y(c) \end{bmatrix} = \begin{bmatrix} \Delta L_{cx1} + H_{c1}S_{xc} + H_{c1}\sin(c)S_{zc} \\ \Delta L_{cx2} + H_{c2}S_{xc} + H_{c2}\sin(c)S_{zc} \\ \Delta L_{cy1} - H_{c1}S_{xc} - H_{c1}\cos(c)S_{zc} \\ \Delta L_{cy2} - H_{c2}S_{xc} - H_{c2}\cos(c)S_{zc} \end{bmatrix} \quad 8$$

It can be obtained by matrix inversion, why singular matrices have not been taken into consideration( $c \neq 0$ ).

$$\xi_x(c) = \frac{\cos(c)(\Delta L_{cy1} - \Delta L_{cy2}) + \sin(c)(\Delta L_{cx2} - \Delta L_{cx1}) - \cos(c)S_{xc} - \sin(c)S_{zc} - S_{xc}}{H_{c1} - H_{c2}} \quad 9$$

$$\xi_y(c) = \frac{\cos(c)(\Delta L_{cx2} - \Delta L_{cx1}) + \sin(c)(\Delta L_{cy2} - \Delta L_{cy1}) - \cos(c)S_{xc} + \sin(c)S_{zc}}{H_{c1} - H_{c2}} \quad 10$$

$$\delta_y(c) = \frac{\sin(c)(H_{c2}\Delta L_{cx1} - H_{c1}\Delta L_{cx2}) + \cos(c)(H_{c1}\Delta L_{cy2} - H_{c2}\Delta L_{cy1})}{H_{c1} - H_{c2}} \quad 11$$

$$\delta_x(c) = \frac{\cos(c)(H_{c1}\Delta L_{cy2} - H_{c2}\Delta L_{cy1}) + \sin(c)(H_{c1}\Delta L_{cx2} - H_{c2}\Delta L_{cx1})}{H_{c1} - H_{c2}} \quad 12$$

(3) C-Z measurement

In the C-Z detection model, double bar ball will be utilized to measure the displacement error of C-axis. When the C-axis rotates, the double bar ball will expand and contract in the axial direction. Considering that axis C is alone without the other axes involved during the motion process, the axial displacement increment  $\Delta L_{cz}$  is the error source parameter  $\delta_z(c)$ . Thus  $\delta_z(c)$  can be obtained as

$$\Delta L_{cz} = D'_{cz} - D_{cz} = \delta_z(c) \quad 13$$

Thus, based on obtained constant, the five PDGs of C axis will be identified totally.

### 4. Results of calculation and simulation

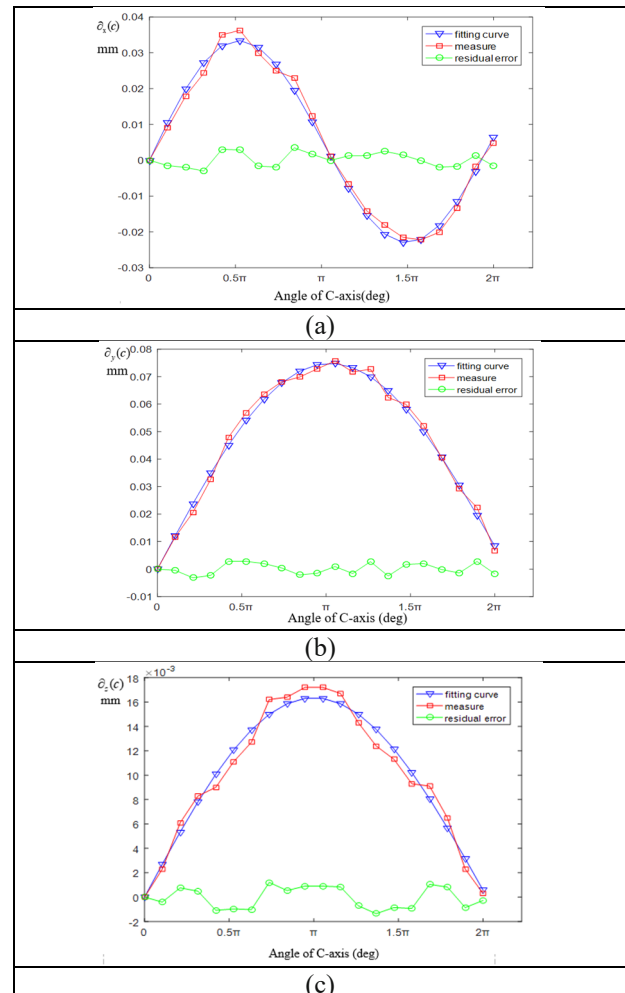
In the third part, a method of geometric error identification of rotation axis is proposed, which only taken picking two points at random into consideration. However, considering the factor that the error of the guide machine varies with the movement of the machine, a comprehensive identification method for the rotary axis is proposed. For the first stage, all 16 geometric errors were described as third-orders truncated Fourier polynomials, and the identification of the polynomial coefficients were based on the selection of measurement points through an observability index. For the second stage, based upon the identification results of stage one, an integrated geometric error identification model of rotating axis is proposed to improve the identification accuracy.

In the simulations, the identification accuracy of different sets of measurement points was compared. The results of identified PDGs are illustrated in Fig. 4, which are fitted by third orders truncated Fourier series. From these, it can be seen that for both the predicted set and the measured sets of points, the motion positions of C-axis covered the entire measurement workspace and ensured a valid

identification accuracy obtained from these sets of measurement points. The red lines represent the fitting curve of measured results, the blue lines represent the predicted results, and the green lines represent residual errors which are calculated by the subtraction between the measured error data and the predicted error data. It is obvious that the predicted values gets close to the measured values by comparing with the measured results. The values of R-square were about fitting curve shown in Table.1 that the maximum value of R-square gets to 0.976. As a matter of fact, the identification method used in this paper possesses less term numbers, smaller fitting residuals, and higher fitting accuracy.

**Table 1** The R-square of five PDGs

PDGE <sub>s</sub>	$\delta_x(c)$	$\delta_y(c)$	$\delta_z(c)$	$\xi_x(c)$	$\xi_y(c)$
R-square value	0.973	0.969	0.976	0.962	0.963



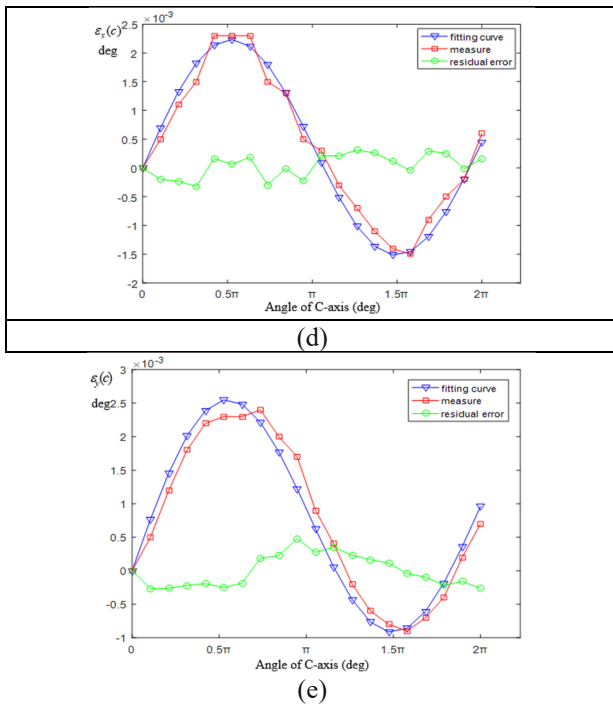


Fig.4. Result of identification

## 5. Conclusion

This paper has proposed a novel and efficient on-machine measurement methodology for identification and prediction of the five PDGs of the rotary axes on a five-axis machine tool by using double ball bar. Error identification model was built based on the multi-body system theory and HTM during the test by measuring length change of double ball bar in the three measure model. In this model, the PDGs of C-axis have been identified completely. Meanwhile fueled by the uncertainty of PDGs, a novel geometric error prediction approach has been devoted to support us to confirm the geometric error conveniently.

## References

1. Tsutsumi M, Saito A (2003) Identification and compensation of systematic deviations particular to 5-axis machining centers. *Int J Mach Tool Manuf* 43(8):771–780
2. Qingzhao Li, Wei Wang Measurement method for volumetric error of five-axis machine tool considering measurement point distribution and adaptive identification process *International Journal of Machine Tools & Manufacture* 147 (2019) 103465
3. M. Tsutsumi, A. Saito, Identification of angular and positional deviations inherent to 5-axis machining centers with a tilting-rotary table by simultaneous four axis control movement, *Int. J. Mach. Tools Manuf.* 44 (12–13) (2004) 1333–1342
4. Y. Abbaszadeh-Mir, J.R.R. Mayer, G. Cloutier, C. Fortin, Theory and simulation for the identification of the link geometric errors for a five-axis machine tool using a telescoping magnetic ball-bar, *Int. J. Prod. Res.* 40 (18) (2002) 4781–4797
5. S.H.H. Zargarbashi, J.R.R. Mayer, Assessment of machine tool trunnion axis motion error using magnetic double ballbar, *Int. J. Mach. Tools Manuf.* 46 (14) (2006) 1823–1834
6. S. Weikert, A new device for accuracy measurements on five axis machine tools, *CIRP Ann.-Manuf. Technol.* 53 (1) (2004) 429–432.
7. S. Ibaraki, C. Oyama, H. Otsubo, Construction of an error map of rotary axes on a five-axis machining center by static r-test, *Int. J. Mach. Tools Manuf.* 51 (3) (2011) 190–200
8. S.H.H. Zargarbashi, J.R.R. Mayer, Single setup estimation of a five-axis machine tool eight link errors by programmed end point constraint and on the fly measurement with capball sensor, *Int. J. Mach. Tools Manuf.* 49 (10) (2009) 759–766
9. C.F. Hong, S. Ibaraki, C. Oyama, Graphical presentation of error motions of rotary axes on a five-axis machine tool by static r-test with separating the influence of squareness errors of linear axes, *Int. J. Mach. Tools Manuf.* 59 (2012) 24–33.
10. Lee KI, Yang SH (2013) Robust measurement method and uncertainty analysis for position-independent geometric errors of a rotary axis using a double ball-bar. *Int J Precis Eng Manuf* 14(2):231–239